

## ADAPTIVE NEURO FUZZY INFERENCE SYSTEM USED TO CLASSIFY THE FIVE MAJOR TYPES OF BRAIN TUMORS

\*<sup>1</sup>Shawni Dutta and <sup>2</sup>Prof. Samir Kumar Bandyopadhyay

<sup>1</sup>Department of Computer Science, The Bhawanipur Education Society College, Kolkata, India.

<sup>2</sup>Academic Advisor, The Bhawanipur Education Society College, Kolkata, India.

Article Received on 06/07/2020

Article Revised on 27/07/2020

Article Accepted on 17/08/2020

### \*Corresponding Author

**Shawni Dutta**

Department of Computer Science, The Bhawanipur Education Society College, Kolkata, India.

### ABSTRACT

Life threatening diseases in both male and female are Brain tumor, stroke, hemorrhage and multiple sclerosis (MS). The most common and widespread disease among these brain diseases is Brain tumor. Early and accurate diagnosis of brain lesion is vital for determining accurate treatment and prognosis. However, the diagnosis is a very

challenging task and can only be performed by specialists in neuroradiology. In this paper, initially MRI image is taken as input and is normalized. The second stage includes extraction of feature vectors from the image which results in reducing redundancy of data to serve as the input to the classifier. The classifier extracted vector as features to produce classified output. The methodology performed very efficiently and accurately. Proposed work exhibits the application of Fuzzy Inference System (FIS) based classifier known as Adaptive Neuro Fuzzy Inference System (ANFIS) to successfully classify the five major types of brain tumors.

**KEYWORDS:** Brain Tumor, Glioma, Meningioma, Metastatic adenocarcinoma, Metastatic bronchogenic carcinoma, Sarcoma.

### INTRODUCTION

Brain tumors forms the second most cause for cancer related deaths in children and adults. A tumor can be graded in to several stages in accordance to the analysis of abnormality of the tumor cells and tissues. This grading gives us the acute probability of tumor growth in size

and its spreading. Tumor grade can be determined using biopsy. It is to be noted that grading of tumor is not same as cancer stages. The accurate diagnosis of brain tumors types is sometimes very difficult due to its high complexity and there are large variations. Five major types of brain tumors: 1) Glioma, 2) Meningioma, 3) Metastatic adenocarcinoma, 4) Metastatic bronchogenic carcinoma, and 5) Sarcoma are considered for computerized classification.<sup>[1]</sup> A database has been created that contains images associated with its corresponding class label. Images from this database were used in testing and training the classifiers.

In the first stage MRI image is taken as input and is normalized. The second stage includes extraction of feature vectors from the image which results in reducing redundancy of data to serve as the input to the classifier. The classification stage classifies the important feature for detection of tumour.<sup>[2]</sup>

### Literature Reviews

The most important aim of brain MRI analysis is to extract clinical information that would improve diagnosis and treatment of disease. Extracting clinical information requires detection and segmentation of normal and abnormal tissues. In the recent days CAD system is used to enhance diagnostic capabilities of physicians and reduce the time required for accurate diagnosis.<sup>[3]</sup>

Computer aided detection of brain tumors, stroke lesions, hemorrhage lesions, and multiple sclerosis lesions are the most difficult issues in field of abnormal tissues segmentations because of many challenges.<sup>[4-5]</sup> The brain injuries are of varied shapes and also distort other normal and healthy tissues structures. Intensity distribution of normal tissues is very complicated and there exist some overlaps between different types of tissues. Over the last decade various approaches have been proposed for the same. Some researcher work on segmentation problem through machine learning methods. It is meant a well trained model that can determine whether a pixel belongs to a normal or abnormal tissue. Brain tumors are one of the most common brain diseases, so detection and segmentation of brain tumors in MRI are important in medical diagnosis.<sup>[6]</sup>

Supports Vector Machines (SVMs) are popular tools for classification by maximize the margin between classes of data that is independent and identically distributed. A SVM classification to classify the brain into the abnormal and normal classes using T1- weighted

and contrast enhanced T1- weighted images.<sup>[7]</sup> This system used patient-specific training and compared classification of normal and abnormal using SVM classifier. It used the standard 2-class method and the more recent 1-class method.<sup>[8]</sup> The SVM method has the advantage of generalization and working in high dimensional feature space. It assumes that data are independently and identically distributed. Segmenting medical images with in-homogeneity and noise are creating problems of such classifiers.

Artificial neural network (ANN) is one of the powerful artificial intelligence techniques that have the capability to learn from a set of data and construct weight matrices to represent the learning patterns. Each node in an ANNs is capable of performing elementary computations.<sup>[9]</sup> Neural networks represent both linear and nonlinear relationships and have the ability to learn these relationships directly from the data. Traditional linear models are simply inadequate since it contains nonlinear characteristics.<sup>[10]</sup> Because of the many interconnections used in a neural network, spatial information can be easily incorporated into its classification procedures.

Neural networks execute very well on complicated, difficult, multivariate non-linear domains, such as tumour, stroke, and hemorrhage segmentation where it becomes more difficult to use decision trees, or rule-based systems. They also perform a little better on noisy fields and there is no need to assume a fundamental data allocation such as usually done in statistical modelling.<sup>[11]</sup>

Patients with brain tumours comprise a heterogeneous group with regard to age, symptom severity and prognosis. One should consider the best possible timing of surgery or oncological therapy. The risk to the patient increases if treatment is delayed.

### **Data Set**

Dataset is a collection of similar and related data stored for processing. Further this can be defined as a collection of data that contains individual data units organized in a specific format. A data set generally contains a collection of a number of types of data. Medical dataset can be defined as a collection of pieces of information, especially those that are part of a collection to be used for the the diagnosis of diseases. Brain MRI images of normal and abnormal from a real human brain MRI dataset are applied in the proposed system. Axial, T2, T1, and PD MR Brain images are used as dataset. Images from the Harvard Medical School.<sup>[5]</sup> website used for normal and abnormal brain images: (a) tumors, (b) strokes, (c)

hemorrhage, and (d) MS. Standard simulations from brainweb database<sup>[12]</sup> include parameter setting fixed to 3 modalities (T1, T2 and PD), 5 slice thicknesses (1, 3, 5, 7 or 9mm), and defining a volume (x, y, z). GM, WM and CSF are tissue classes. The brain model used to generate the simulations can be also employed as ground truth. Another public domain dataset are used to conducting similar research. MRI database, available in the Internet, for different brain abnormality of MR images are also used.<sup>[13]</sup> All mentioned dataset are used to evaluate the performance.

These detections are based on the diagnosis of radiologists. The size of tumour is also classified according to the type of tumour present.

### Proposed Method

Tumour detected MRI of brain slices is selected for classification. Artifacts and skull elimination is used to remove unnecessary regions of MRI. Next these are normalized to a range for feature extraction process. In the classification step, the model is first trained using training dataset obtained from the image database which also defines the class labels being used. After performing the training on set of existing known data set then test the data for appropriate classes that help in correct medical decision making and diagnosis of brain tumour. The brief implementation of the technique has been shown in figure 1.

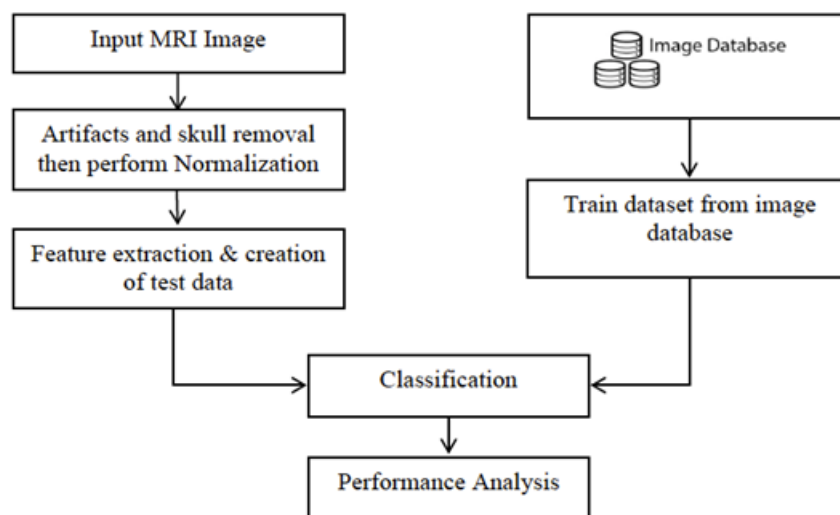


**Figure 1: Workflow of the tumour classification.**

### Features selection

Histogram of an image represents the concise statistical information contained in the image. Now consider that  $f(x, y)$  is the function that represents the intensity level for each pixel (x,

$y$ ) in the image, where  $x = 1, 2, \dots, A$  and  $y = 1, 2, \dots, B$ . Grey-level histogram calculation involves each individual pixel. Probability density for each occurring pixel intensity level  $0, 1, \dots, N - 1$  is calculated dividing them with  $h(i)$  by total number of pixels. This can be represented as:

$$p(i) = \frac{h(i)}{AB} \quad \text{for } i = 0, 1, \dots, N - 1 \quad (1)$$

$$h(i) = \sum_{x=1}^A \sum_{y=1}^B \delta(f(x, y), i)$$

$$x=1 \quad y=1 \quad (2)$$

Here  $h(i)$  is the intensity level histogram function for the whole image and for each intensity level  $i$ .

Here we have taken  $\delta(i, j)$  as the kronecker delta function that can be given as:

$$\delta(i, j) = \begin{cases} 1, & i = j \\ 0, & i \neq j \end{cases}$$

Various useful parameters can be derived from the histogram to describe the statistical information about the image. These parameters are taken to be parameters for feature extraction. They are described below:

*Mean:* The average value of intensity of the image and can be given as:

$N - 1$

$$\mu = \sum_{i=0}^{N-1} i \cdot p(i)$$

$$i = 0 \quad (4)$$

*Variance is defined as:*

$N - 1$

$$\sigma^2 = \sum_{i=0}^{N-1} (i - \mu)^2 p(i)$$

$$i = 0 \quad (5)$$

*Skewness*: Gives us the measure of the amount of symmetry of the histogram around mean. It can be given by:

$$\mu_3 = \frac{1}{N} \sum_{i=0}^{N-1} (i - \mu)^3 p(i) \quad (6)$$

*Kurtosis*: Measures the flatness in the histogram and is given by:

$$\mu_4 = \frac{1}{N} \sum_{i=0}^{N-1} (i - \mu)^4 p(i) - 3 \quad (7)$$

*Entropy*: Represents the uniformity of the histogram and is given by:

$$H = - \sum_{i=0}^{N-1} p(i) \log_2 [p(i)] \quad (8)$$

*Energy*: Represents the mean of squared value of the pixel intensity and can be given as:

$$E = \sum_{i=0}^{N-1} [p(i)]^2 \quad (9)$$

All the mentioned parameters give us the information extracted from the local image histograms and can be used for texture segmentation. The normalization as given in previous step results in better texture discrimination accuracy. One of the major advantages of using these parameters is that they are simple, but they are not able to completely characterize texture. To solve this joint probability distributions of pixel pairs are required. Using this definition second order histogram known as grey-level co-occurrence matrix  $h_{d\theta}(i, j)$  has been considered.

The image matrix is divided by the total number of neighbouring pixels  $R(d, \theta)$  in the image, the resulting image becomes the joint probability  $p_{d\theta}(i, j)$  for two pixels with distance  $d$  between them and along the direction  $i$  and  $j$ . Value for  $d = 1, 2$  and  $\theta = 0, 45, 90, 135$  are normally used. For a given image with intensity function  $f(x, y)$  and  $N$  discrete intensity values, matrix  $h_{d\theta}(i, j)$  and defining the parameters  $i$  and  $j$  as:

$$f(x_1, y_1) = I \text{ and } f(x_2, y_2) = j \quad (10)$$

$$\text{Where } (x_2, y_2) = (x_1, y_1) + (d \cos \theta, d \sin \theta) \quad (11)$$

This results in a matrix dimension equal to the number of intensity levels and for each distance  $d$  and orientation  $\theta$ . Thus the co-occurrence matrix contains  $N^2$  elements that can be considered as a reduced set of features. Some of the parameters that can be derived from the matrix can be given as follows, where  $\mu_x, \mu_y$  and  $\sigma_x, \sigma_y, \sigma_x, \sigma_y$  as the mean and standard deviation derived from this matrix. The parameters are given as:

*Angular second moment (energy):* Energy also means uniformity, or angular second moment. The more homogeneous the image is, the larger the value. The image is believed to be a constant image when energy equals to 1.

$$\sum_{i=0}^{N-1} \sum_{j=0}^{N-1} [p(i, j)]^2 \quad (12)$$

*Correlation:* This feature measures how correlated a pixel is to its neighbourhood. It is defined as,

$$\frac{\sum_{i=0}^{N-1} \sum_{j=0}^{N-1} ij p(i, j) - \mu_x \mu_y}{\sigma_x \sigma_y}$$

*Inertia (Contrast)*: Contrast measures the quantity of local changes in an image. It reflects the sensitivity of the textures in relation to changes in the intensity. It returns the measure of intensity contrast between a pixel and its neighbourhood.

$$\sum_{i=0}^{N-1} \sum_{j=0}^{N-1} (i-j)^2 p(i,j) \quad (14)$$

*Absolute value*: Measures the intensities of the image.

$$\sum_{i=0}^{N-1} \sum_{j=0}^{N-1} i-j p(i,j) \quad (15)$$

*Inverse Difference*: Influenced by the homogeneity of the image. The result is a low inverse difference value for inhomogeneous images, and a relatively higher value for homogeneous images.

$$\sum \sum p(i,j)^2$$

$$\sum_{i=0}^{N-1} \sum_{j=0}^{N-1} 1 + (i-j) \quad (16)$$

*Entropy*: It denotes the randomness of intensity image.

$$H = -\sum_{i=0}^{N-1} \sum_{j=0}^{N-1} p(i,j) \log_2 [p(i,j)] \quad (17)$$

Using above discussed parameters feature vector generates that can help in classification of the input image into the predetermined class label.

### Classification

Classification step occurs in two consecutive steps: learning phase and testing phase. The first one is known as training phase. It is the first step in classification. In this step it needs to build a model that can successfully classify a dataset. Back propagation algorithm is an optimization procedure based on gradient descent that adjusts the weights to reduce the system error. During the learning phase, input patterns are presented to the network and the network parameters are changed to bring the actual outputs closer to the desired target values. These outputs are compared to the target values. Any difference indicates an error. These errors are some scalar function of the weights. So the weights are to be adjusted for reducing the errors. This error function is the sum of square differences of the outputs and targets. Thus, the errors computed at the output layer are used to adjust the weights between the last hidden layer and the output layer.

The Artificial Neural Network System (ANFIS) uses fuzzy rules and fuzzy reasoning that is based on fuzzy set theory. It can also be said that fuzzy stands out to be a form of multi valued logic. FIS is based upon the concepts of fuzzy set theory, fuzzy if-then rules and fuzzy reasoning. In case of fuzzy if-then rules which take the following form:

$$\text{if } x \text{ is } A \text{ then } y \text{ is } B \quad (18)$$

Here  $A$  and  $B$  are linguistic values which is defined by fuzzy sets on the universe of discourse of  $X$  and  $Y$  respectively. The statement “  $x$  is  $A$  ” is called the antecedent and the statement “  $y$  is  $B$  ” is called the consequence. The relation between two variables  $x$  and  $y$  in which the fuzzy rule defined as a binary relation  $F$  on the product space  $X \times Y$ . A fuzzy model can assume the following form of fuzzy rules:

$$\text{if } x \text{ is } A \text{ and } y \text{ is } B \text{ then } z = f(x, y) \quad (19)$$

Here  $A$  and  $B$  are fuzzy rules and  $z = f(x, y)$  is a crisp on the input variables  $x$  and  $y$ . A two input ANFIS has been shown in Figure 2.

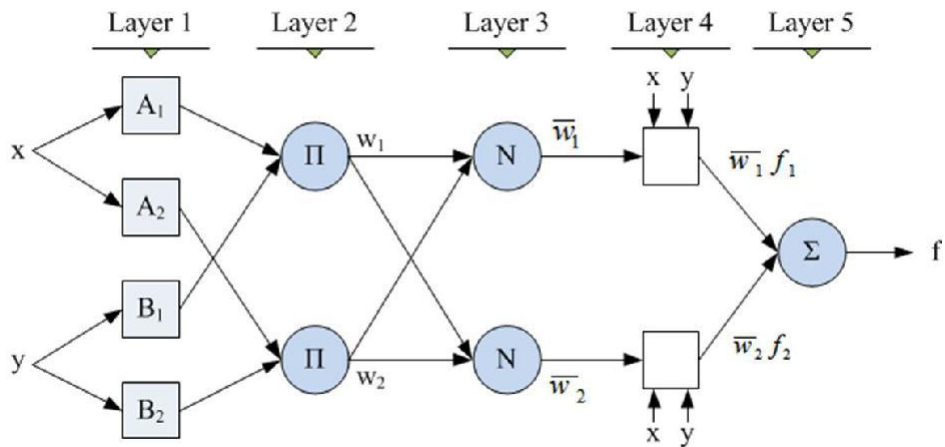


**Figure 2: ANFIS architecture equivalent to fuzzy inference system.**

Each  $i^{\text{th}}$  node in the a particular layer  $l$  takes an input from the previous layer and produces an output  $O_{l,i}$ . Now mapping for each individual layer is presented below:

For layer 1 we take  $l = 1$  and output as  $O_{1,i}$  for each  $i^{\text{th}}$  node in this layer. Every node in this layer is considered to be an adaptive node where the node function can be described as:

$$O_{1,i} = \begin{cases} \varphi_{A_i}(x) & \text{for } i = 1,2 \\ \varphi_{B_i}(y) & \text{for } i = 3,4 \end{cases}$$

Here  $x$  or  $y$  is the input variable to node  $i$  and each node is assigned a linguistic label  $A_i$  or  $B_{i-2}$  to it. Here  $\varphi_A(x)$  denotes the membership function for  $A$  and can be any valid parameterized function that depends on a parameter set. This parameter set can also be called as premise parameters.

In the next layer (Layer 2) the output for the incoming signal can be defined by:

$$O_{2,i} = w_i = \varphi_{A_i}(x)\varphi_{B_i}(y) \text{ for } i = 1,2 \quad (21)$$

This output represents the firing strength of a rule.

Layer 3 calculate the normalized firing strengths for every  $i^{\text{th}}$  node and can be calculated as the ratio between the firing strength of that layer to the sum of all firing rules in that layer as:

$$O_{3,i} = w_i = 2^{w_i}$$

$$\sum w_i = 1 \quad (22)$$

In layer 4 computes the output considering the parameter set embedded in the membership function. The parameters in this set are referred as consequent parameters. The node function for every  $i^{\text{th}}$  node can be given as:

$$O_{4,i} = w_i f_i(x, y) \quad (23)$$

In the last layer (layer 5) each of the node is assigned with a fixed node label  $\Sigma$ . Each node computes the summation of all incoming signals as outputs as:

$$O_{5,i} = \sum_i w_i f_i(x, y) = \frac{\sum w_i f_i(x, y)}{\sum w_i}$$

In this model it has been observed that if a particular tuple does not match with the established fuzzy rules defined in the model, the classifier tries to give a result that is outside the solution set. This is helpful in determining a new type of tumour.

The images are normalized to the feature vector containing 12 features are extracted from the slices. Each of the feature vector forms an input tuple to the classifier. This vector is generated for 20 input slices shown in Figure 3 (Collected from hospitals) has been illustrated by Table 1 and Table 2.

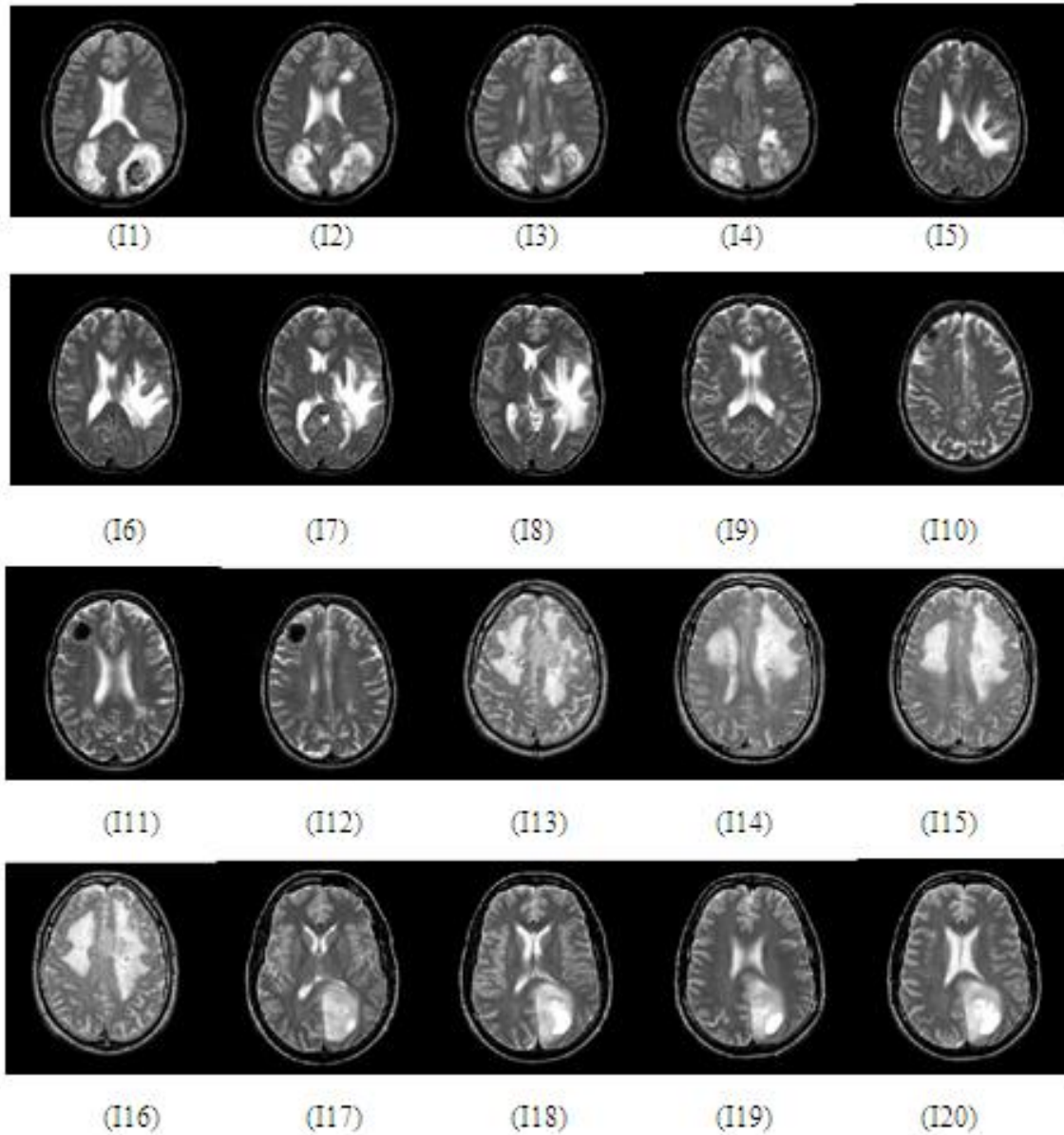


**Figure 3: 20 input slices passed through the normalization and feature extraction processes for classification. After classification it is found that slices I1-I4 are Type 1 (Sarcoma); slices I5-I8 are Type 2 (Meningioma); slices I9-I12 are Type 3 (Metastatic adenocarcinoma); slices I13-I16 are Type 4 (Metastatic bronchogenic carcinoma); slices I17-I20 are Type 5 (Glioma).**

Each of the generated feature vector from the normalized grayscale image are calculated from 1<sup>st</sup> order histogram based features and features from Gray Level Co-occurrence Matrix. Each of the functions derives a single valued element in the feature extraction matrix for each of the 20 slices that is represented in Table 1 and Table 2.

**Table 1: Feature vector from the normalized grayscale MR image.**

| Image sequence | Mean    | Variance | Skewness | Kurtosis | Energy | Entropy |
|----------------|---------|----------|----------|----------|--------|---------|
| 1              | 15.5399 | 446.433  | 0.000108 | 0.000127 | 0.2816 | 3.6817  |
| 2              | 14.7607 | 427.681  | 0.000126 | 0.000151 | 0.2933 | 3.5751  |
| 3              | 15.5426 | 447.411  | 0.000108 | 0.000127 | 0.2810 | 3.6939  |
| 4              | 15.3294 | 434.847  | 0.000116 | 0.00014  | 0.2762 | 3.7014  |
| 5              | 15.9980 | 466.920  | 0.0001   | 0.000118 | 0.2718 | 3.8210  |
| 6              | 16.2995 | 455.317  | 0.000972 | 0.000117 | 0.2540 | 3.8918  |
| 7              | 16.8535 | 461.050  | 0.000906 | 0.00011  | 0.2365 | 3.9722  |
| 8              | 15.2010 | 463.274  | 0.000113 | 0.000132 | 0.2981 | 3.6796  |
| 9              | 13.6257 | 406.182  | 0.00015  | 0.000185 | 0.3333 | 3.2856  |
| 10             | 13.9531 | 413.331  | 0.000143 | 0.000175 | 0.3219 | 3.4029  |
| 11             | 13.1538 | 400.748  | 0.000161 | 0.000200 | 0.3529 | 3.2298  |
| 12             | 14.2234 | 417.177  | 0.000137 | 0.000165 | 0.3123 | 3.4526  |
| 13             | 13.6782 | 420.489  | 0.000142 | 0.000167 | 0.3506 | 3.2687  |
| 14             | 13.5103 | 417.582  | 0.000144 | 0.000169 | 0.3583 | 3.1849  |
| 15             | 13.2064 | 412.893  | 0.000151 | 0.000178 | 0.3698 | 3.1134  |
| 16             | 12.3658 | 388.257  | 0.000181 | 0.000226 | 0.3857 | 3.0153  |
| 17             | 12.9241 | 397.207  | 0.000167 | 0.00021  | 0.3573 | 3.2094  |
| 18             | 13.5875 | 407.496  | 0.000151 | 0.000185 | 0.3342 | 3.3352  |
| 19             | 14.2193 | 425.415  | 0.000137 | 0.000164 | 0.3174 | 3.4692  |
| 20             | 14.9834 | 443.361  | 0.000118 | 0.000138 | 0.3040 | 3.5664  |

**Table 2: Feature vector of normalized grayscale MR image.**

| Image sequence | Contrast | Correlation | Energy | Homogeneity | Inverse difference | Absolute value |
|----------------|----------|-------------|--------|-------------|--------------------|----------------|
| 1              | 0.3334   | 0.3878      | 0.4131 | 0.8726      | 56710.6            | 17910          |
| 2              | 0.3190   | 0.3833      | 0.4379 | 0.8774      | 57036.6            | 17210          |
| 3              | 0.3415   | 0.3862      | 0.4071 | 0.8697      | 56512.8            | 18328          |
| 4              | 0.3547   | 0.3508      | 0.4112 | 0.8659      | 56247.2            | 18914          |
| 5              | 0.3618   | 0.3884      | 0.3971 | 0.8663      | 56246              | 18994          |
| 6              | 0.3499   | 0.3785      | 0.3871 | 0.8652      | 56218.6            | 18910          |
| 7              | 0.3697   | 0.3640      | 0.3731 | 0.8592      | 55806.6            | 19812          |
| 8              | 0.3610   | 0.3920      | 0.4227 | 0.8712      | 56534.6            | 18504          |
| 9              | 0.2931   | 0.3803      | 0.4756 | 0.8861      | 57632.2            | 15936          |
| 10             | 0.2984   | 0.3755      | 0.4668 | 0.8831      | 57439.6            | 16314          |
| 11             | 0.2885   | 0.3749      | 0.4930 | 0.8896      | 57854              | 15516          |
| 12             | 0.3019   | 0.3595      | 0.4589 | 0.8800      | 57245.4            | 16676          |
| 13             | 0.2558   | 0.4260      | 0.4907 | 0.8970      | 58395.4            | 14258          |
| 14             | 0.2565   | 0.4179      | 0.4908 | 0.8972      | 58406              | 14248          |
| 15             | 0.2443   | 0.4349      | 0.5019 | 0.9011      | 58674.6            | 13668          |
| 16             | 0.2395   | 0.4074      | 0.5274 | 0.9029      | 58796.6            | 13412          |
| 17             | 0.2881   | 0.3883      | 0.4918 | 0.8902      | 57893.2            | 15446          |
| 18             | 0.2936   | 0.3933      | 0.4727 | 0.8867      | 57670.4            | 15878          |
| 19             | 0.3158   | 0.3685      | 0.4617 | 0.8804      | 57227              | 16858          |
| 20             | 0.3164   | 0.3804      | 0.4429 | 0.8786      | 57115.6            | 17050          |

Each tuple contains its class label which denotes its tumour type which is used to build IF-THEN rules to generate the FIS. ANFIS is trained network that is used to generate the class label for the input slices. The class labels mentioned here were taken accordingly as: Class 1 = Sarcoma, Class 2 = Meningioma, Class 3 = Metastatic adenocarcinoma, Class 4 = Metastatic bronchogenic carcinoma, Class 5 = Glioma. The classifier gives fuzzy numbers as output which is de-fuzzified to get the crisp actual class labelled values.

### Performance measurement

Performance is measured by comparing the actual class labels and the predicted class labels for each of the individual classifiers. In statistical analysis of classification, the F-score or F-measure is a measure of a test's accuracy. Performance measurement metrics value of 5 major tumour types as different class has been shown in Table 3.

**Table 3: Performance measurement metrics value of 5 major tumour types.**

| Metric                      | Class 1 | Class 2 | Class 3 | Class 4 | Class 5 |
|-----------------------------|---------|---------|---------|---------|---------|
| True Positive (TP)          | 37      | 43      | 32      | 29      | 48      |
| False Negative (FN)         | 4       | 4       | 5       | 2       | 4       |
| False Positive (FP)         | 3       | 3       | 2       | 6       | 5       |
| True Negative (TN)          | 164     | 158     | 169     | 171     | 151     |
| Sensitivity( $TP/(TP+FN)$ ) | 0.902   | 0.914   | 0.864   | 0.935   | 0.923   |
| Specificity( $TN/(FP+TN)$ ) | 0.982   | 0.981   | 0.988   | 0.966   | 0.967   |
| Precision( $TP/(TP+FP)$ )   | 0.925   | 0.934   | 0.941   | 0.828   | 0.905   |
| Accuracy( $(TP+TN)/(P+N)$ ) | 0.966   | 0.966   | 0.966   | 0.961   | 0.956   |
| F score( $2TP/(2P+FP+FN)$ ) | 0.913   | 0.924   | 0.901   | 0.878   | 0.914   |

The performance of the classifiers is evaluated in terms of sensitivity, specificity, precision, accuracy and F score. The average value of sensitivity is 0.90815166, average value of specificity is 0.977151379, average value of precision is 0.907038177, average value of accuracy is 0.963461538, and average value of F score is 0.906558695 for an ANFIS. ROC curve of proposed system has been shown in Figure 4.

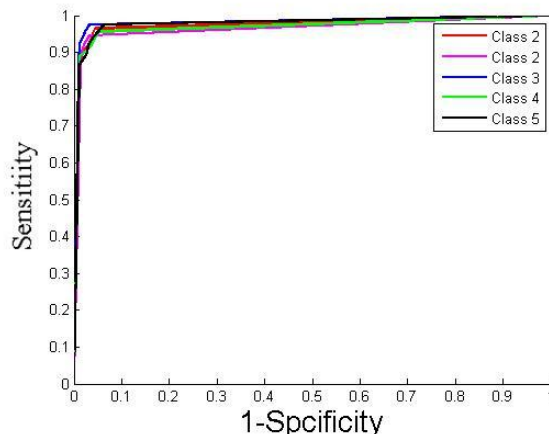


**Figure 4: ROC curve for brain tumour classification.**

## CONCLUSIONS

The accuracy of classifier obtained 96.34% on Harvard benchmark dataset for both contrast and non-contrast images. The models are classified by ANFIS to enhance generalization capability. Automation of a model for computing an estimate of the type of tumor are verified by a radiologist. The proposed system can help the physicians to identify the type of brain tumors for further treatment.

## REFERENCES

1. E. E. M. Azhari, M. M. M. Hatta, Z. Z. Htike, and S. L. Win, "Tumor detection in medical imaging: a survey," *International Journal of Advanced Information Technology*, 2014.
2. J. Liu, M. Li, J. Wang, F. Wu, T. Liu, and Y. Pan, "A survey of MRI based brain tumor segmentation methods," *Tsinghua Science and Technology*, 2014.
3. S. Shen, W. Sandham, M. Granat, and A. Sterr, "MRI fuzzy segmentation of brain tissue using neighborhood attraction with neural-network optimization," *IEEE Transaction on Information Technology in Biomedicine*, 2005.
4. D. L. Pham, C. Xu, and J. L. Prince, "Current methods in medical image segmentation," *Annual Review of Biomedical Engineering*, 2000.
5. T. Logeswari and M. Karnan, "An improved implementation of brain tumor detection using segmentation based on hierarchical self-organizing map," *International Journal of Computer Theory and Engineering*, 2010.
6. N. B. Bahadure, A. K. Ray, and H. P. ethi, "Image analysis for MRI based brain tumor detection and feature extraction using biologically inspired BWT and SVM," *International Journal of Biomedical Imaging*, 2017.

7. A. Hanuman and K. Sooknanan, "Brain tumor segmentation and volume estimation from T1-contrasted and T2 MRIs," *International Journal of Image Processing (IJIP)*, 2018.
8. A. Hazra, A. Dey, and S. K. Gupta, M. A. Ansari, "Brain tumor detection based on segmentation using MATLAB," in *Proceedings of the International Conference on Energy, Communication, Data Analytics and So- Computing (ICECDS)*, IEEE, Piscataway, NJ, USA, 2017.
9. A. Gujar and C. M. Meshram, "Brain tumor extraction using genetic algorithm," *International Journal on Future Revolution in Computer Science and Communication Engineering (IJFRSCE)*, 2018.
10. S. Pereira, A. Pinto, V. Alves, and C. A. Silva, "Brain tumor segmentation using convolutional neural networks in MRI images," *IEEE Transactions on Medical Imaging*, 2016.
11. I. Kullayamma and A. Praveen Kumar, "Brain tumor segmentation by using ant colony optimization," *International Journal of Scientific Research in Science and Technology*, 2018.
12. Whole Brain Atlas: MR brain image available online, 2013.
13. The EASI MRI Home: MR brain image available online, 2013.  
<http://www.easidemographics.com/cgi-bin/dbmri.asp>.